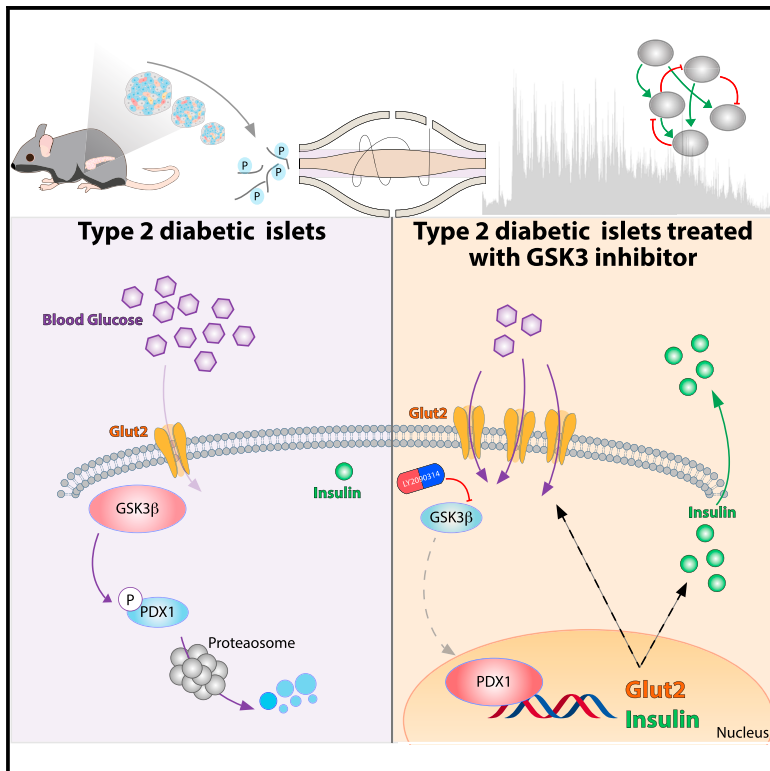# Phosphoproteomics Reveals the GSK3-PDX1 Axis as a Key Pathogenic Signaling Node in Diabetic Islets

Graphical Abstract

Authors

Francesca Sacco, Anett Seelig, Sean J. Humphrey, ..., Piero Marchetti, Jantje Gerdes, Matthias Mann

Correspondence

francesca.sacco@uniroma2.it (F.S.), mmann@biochem.mpg.de (M.M.)

In Brief

Using highly sensitive and streamlined mass spectrometry analyses, combined with bioinformatics, Sacco et al. generated in-depth proteome and phosphoproteome signaling network maps of normal and diabetic murine pancreatic islets. They identified GSK3 as a crucial regulatory node in insulin secretion; GSK3 inhibition restores the ability of diabetic islets to secrete insulin.

Highlights

- Pathogenic signaling pathways are rewired in type 2 diabetic islets

- The GSK3-PDX1 axis is compromised in type 2 diabetic islets

- The GSK3 kinase is a crucial regulator of GLUT2 and insulin expression

- GSK3 inhibition restores the ability of diabetic islets to secrete insulin

CellPress

Phosphoproteomics Reveals the GSK3-PDX1 Axis as a Key Pathogenic Signaling Node in Diabetic Islets

Francesca Sacco,[1,4,*] Anett Seelig,[2] Sean J. Humphrey,[3] Natalie Krahmer,[1] Francesco Volta,[2] Alessio Reggio,[4] Piero Marchetti,[5] Jantje Gerdes,[2] and Matthias Mann[1,6,*]

[1]Proteomics and Signal Transduction, Max-Planck Institute of Biochemistry, 82152 Martinsried, Germany
[2]Helmholtz Diabetes Center (HMGU) and German Center for Diabetes Research (DZD), 85748 Garching, Munich, Germany
[3]School of Life and Environmental Sciences, Charles Perkins Centre, The University of Sydney, Sydney, NSW 2006, Australia
[4]Department of Biology, University of Rome Tor Vergata, 00100 Rome, Italy
[5]Department of Clinical and Experimental Medicine, University of Pisa, 56126 Pisa, Italy
[6]Lead Contact
*Correspondence: francesca.sacco@uniroma2.it (F.S.), mmann@biochem.mpg.de (M.M.)
https://doi.org/10.1016/j.cmet.2019.02.012

SUMMARY

Progressive decline of pancreatic beta cell function is central to the pathogenesis of type 2 diabetes. Protein phosphorylation regulates glucose-stimulated insulin secretion from beta cells, but how signaling networks are remodeled in diabetic islets *in vivo* remains unknown. Using high-sensitivity mass spectrometry-based proteomics, we quantified 6,500 proteins and 13,000 phosphopeptides in islets of obese diabetic mice and matched controls, revealing drastic remodeling of key kinase hubs and signaling pathways. Integration with a literature-derived signaling network implicated GSK3 kinase in the control of the beta cell-specific transcription factor PDX1. Deep phosphoproteomic analysis of human islets chronically treated with high glucose demonstrated a conserved glucotoxicity-dependent role of GSK3 kinase in regulating insulin secretion. Remarkably, the ability of beta cells to secrete insulin in response to glucose was rescued almost completely by pharmacological inhibition of GSK3. Thus, our resource enables investigation of mechanisms and drug targets in type 2 diabetes.

INTRODUCTION

The metabolic syndrome is caused by a complex interplay between genetic, epigenetic, and lifestyle factors, including physical activity and diet (DeFronzo et al., 2015). Type 2 diabetes (T2D) mellitus in particular is a major public health issue, accompanied by a chronic decline of glycemic control. T2D is a highly heterogeneous disorder caused by a complex interplay between insulin resistance and beta cell dysfunction (Ahlqvist et al., 2018; Prasad and Groop, 2015). Growing evidence implicates beta cell dysfunction as a key event during T2D development (Saisho, 2015). Genome-wide association studies (GWASs) have identified multiple risk variants for T2D with a primary role in beta cell function, highlighting their importance in the development of T2D (McCarthy and Hattersley, 2008). However, our knowledge of the molecular mechanisms underlying the development of beta cell dysfunction is still far from complete. A systems-wide understanding of beta cell dysregulation obtained by unbiased methods could contribute to the treatment and prevention of this disease. Large-scale "omics" technologies, particularly transcriptomics but also mass spectrometry (MS)-based proteomics, have been applied to characterize islets isolated from different T2D animal models and human cadavers (El Ouaamari et al., 2015; Hou et al., 2017; Lu et al., 2008; Segerstolpe et al., 2016). While these analyses have provided sets of differentially expressed genes and proteins involved in beta cell failure, by their design they did not capture the crucial signaling alterations

---

Context and Significance

After a meal, insulin is secreted from the pancreas to keep blood glucose levels stable; this process is disrupted in diabetes. The relative rarity of insulin-producing cells contributes to the challenge of understanding the disease, especially from a big-picture perspective. Researchers at the Max-Planck Institute in Martinsried (near Munich) circumvented the abundance issue by utilizing highly sophisticated, large-scale molecular and chemical analyses, combined with detailed bioinformatics, to generate a comprehensive map of the interconnected proteins in healthy and diseased pancreata. They identified GSK3 as an unappreciated player in insulin secretion. Furthermore, drugs that affect GSK3 function are being developed for cancer and show promise for diabetes. This comprehensive pancreas protein map represents a promising resource for further mining for diabetes therapies.
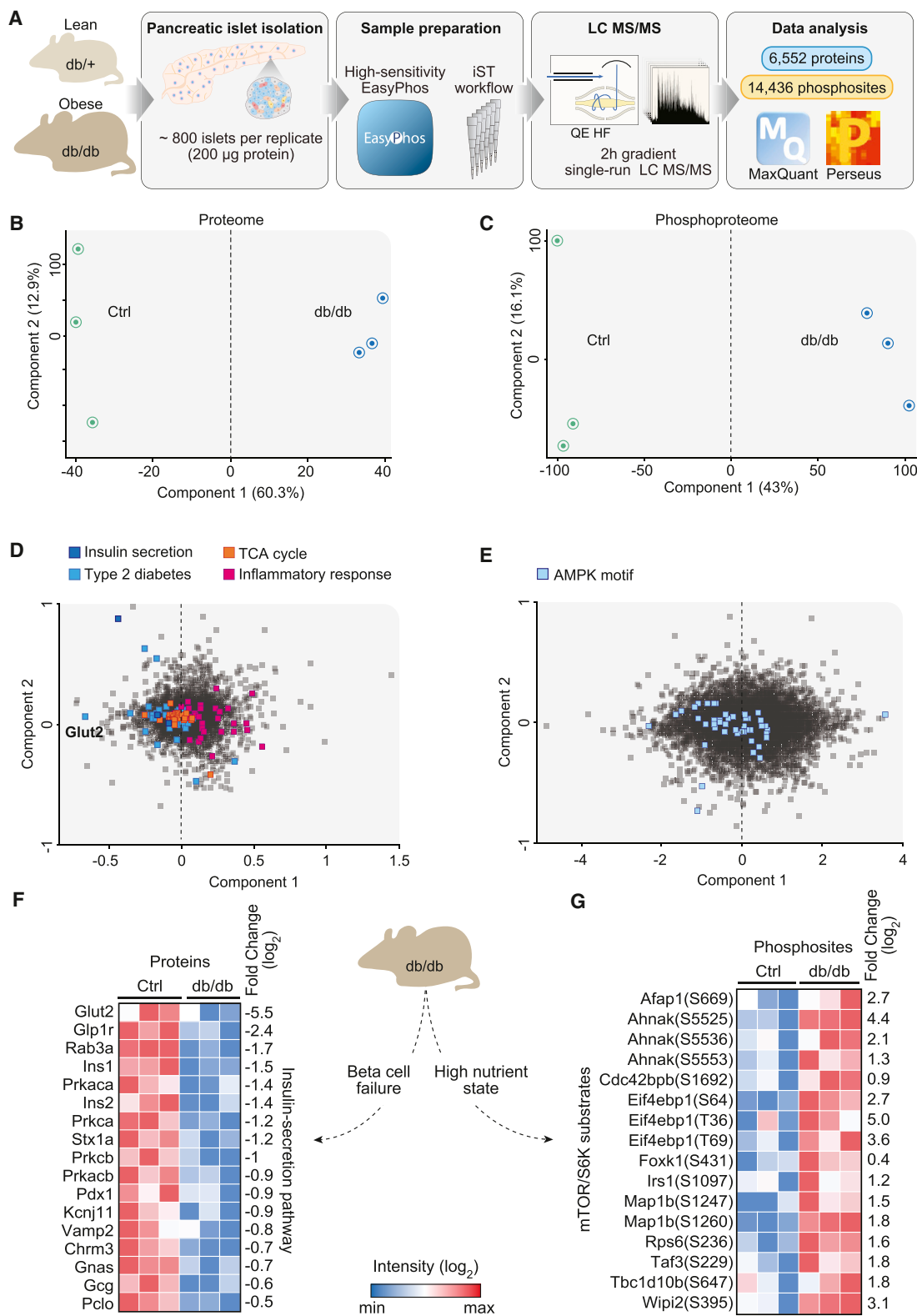

Figure 1. Our Experimental Strategy

(A) Experimental workflow to analyze the proteome and phosphoproteome of pancreatic islets derived from diabetic (db/db) and control (db/+) mice.

(B and C) Principal component analysis (PCA) of proteome (B) and phosphoproteome (C) data.

(legend continued on next page)

at the level of phosphorylation networks. As phosphorylation is a major regulator of insulin secretion and can also be modulated pharmacologically, its global investigation would be highly desirable.

Phosphorylation can be measured at a large scale by proteomics methods, but this involves specific enrichment for phosphorylated peptides and typically requires 100-fold larger input material than proteomics measurements. Consequently, a major obstacle to the global characterization of changes in T2D islets by phosphoproteomics has been the extremely limited amount of material that can be extracted from pancreatic islets. Our group has recently described an MS-based phosphoproteomics workflow, termed "EasyPhos," which enables streamlined and large-scale phosphoproteome analysis over multiple experimental conditions (Humphrey et al., 2015), and we have now improved its sensitivity several-fold (Humphrey et al., 2018). We reasoned that this workflow might enable the in-depth characterization of changes in signaling networks of islets isolated from diabetic compared to control mice. For this purpose, we employed mice that carry an autosomal recessive mutation in the leptin receptor, the standard model in the field. These Lepr$^{db/db}$ mice become obese from 3 to 4 weeks of age and develop hyperglycemia as early as 4–8 weeks (Chen et al., 1996). To obtain a comprehensive view of global signaling network rewiring, we combined phosphoproteomic analysis of diabetic islets with an in-depth characterization of proteome changes. Our analysis revealed a drastic remodeling of the proteome and phosphoproteome, including numerous proteins implicated in insulin secretion control, glucose uptake, and metabolism. To functionally interpret our datasets, we applied a recently developed bioinformatics workflow (Sacco et al., 2016b). This highlighted a novel GSK3-dependent signaling axis contributing to beta cell failure, whose molecular mechanism we investigated in mouse and rat cells as well as in human islet models.

RESULTS AND DISCUSSION

In-Depth Proteomic and Phosphoproteomic Characterization of db/db Islets

To obtain a comprehensive perspective of the mechanisms underlying the insulin secretion failure in diabetic islets, we measured the proteome and phosphoproteome of pancreatic islets isolated from 13-week-old homozygous C57BLKS-Lepr^{db} mice. As expected, these "db/db" mice were obese and hyperglycemic (Figures S1A and S1B). As negative controls, we used age-matched C57BLKS-Lepr^{db}/+ because these heterozygous mice have the same genetic background (hereafter referred to as "Ctrl") (Figure 1A).

We applied a label-free quantification approach by high-resolution liquid chromatography-mass spectrometry (LC-MS) performed in a single-run format on benchtop Orbitrap ("Q Exactive HF") mass spectrometers (Kelstrup et al., 2018; Kulak et al.,

2014). Combined with the latest developments of our EasyPhos workflow, this allowed us to work on single mice for the proteome, whereas we harvested islets from three mice for the phosphoproteome measurements, yielding 200 μg islet proteins. This experimental strategy enabled us to reliably quantify 6,500 proteins (Figure 1A; Table S1) and more than 14,000 different phosphorylation events mapping to 3,821 proteins (Table S2; Figures S2A and S2B). In total, 88% of the phosphoproteome was localized with high confidence to a single amino acid sequence location (Figure S2C), with a median localization probability greater than 0.99 (STAR Methods). These are excellent values, especially when considering the minimal amount of in vivo material, and the fact that no exogenous stimulation was employed.

Both proteome and phosphoproteome measurements where highly accurate and reproducible, with Pearson correlation coefficients of biological replicates ranging between 0.85 (lowest for phosphoproteome measurements) and 0.99 (highest for proteome measurements) (Figures S2D and S2E). In agreement with other MS-based studies (Sharma et al., 2014), the majority of phosphorylation events in pancreatic islets occurred on serine residues (88%), followed by threonine (11%), whereas phosphotyrosines accounted for less than 1% of quantified phosphosites (Figure S3A). Compared to the community database PhosphoSitePlus (Hornbeck et al., 2015), 87% of our quantified phosphosites were identical—a reassuring proportion considering the small sample amount and the depth of the analysis (Figure S3B). Only 268 out of these 10,994 sites are annotated as "regulatory," meaning that the functional role or upstream cognate kinases of the vast majority of phosphorylation events quantified here have not been investigated to date.

Principal component analysis (PCA) of both our proteomic and phosphoproteomic data clearly classified pancreatic islets according to their diabetic status (Figures 1B and 1C). AMPK inhibition, mTOR hyperactivation, and insulin secretion failure are features of type 2 diabetic islets (Blandino-Rosano et al., 2012; Kahn et al., 2006). The drivers of the discrimination (component 1 of the PCA loadings) at the proteome and phosphoproteome level are enriched in annotations with these processes, providing a positive control for our proteomics measurements (Figures 1D and 1E). Likewise, db/db-upregulated proteins were also significantly enriched for inflammation processes (Figure 1D), which are known to correlate with obesity and T2D progression (Donath et al., 2013). Additionally, key proteins involved in insulin secretion were significantly downregulated in db/db islets with log2 fold changes between 0.5- and 5-fold, whereas the phosphorylation of almost all of the mTOR/S6K substrates was increased by similar amounts (FDR < 0.05; Figures 1F and 1G). We conclude that our proteomic screen recapitulated known biology of diabetic islets—particularly regarding the effects of chronic high nutrients on mTOR hyperactivation and insulin secretion failure—while generating a vast resource of previously unknown, regulated events.

(D and E) The loadings of the PCA in (B) and (C) reveal that the proteins (D) and phosphosites (E) responsible for driving the segregation in component 1 are significantly enriched in the GO BPs and Kegg pathways and kinase substrate motifs indicated (FDR < 0.07).

(F) Heatmap of protein levels of the labeled insulin secretion-associated proteins in control and db/db islets.

(G) Heatmap of phosphorylation levels of the indicated phosphosites in control and db/db islets upon drug and glucose treatments.
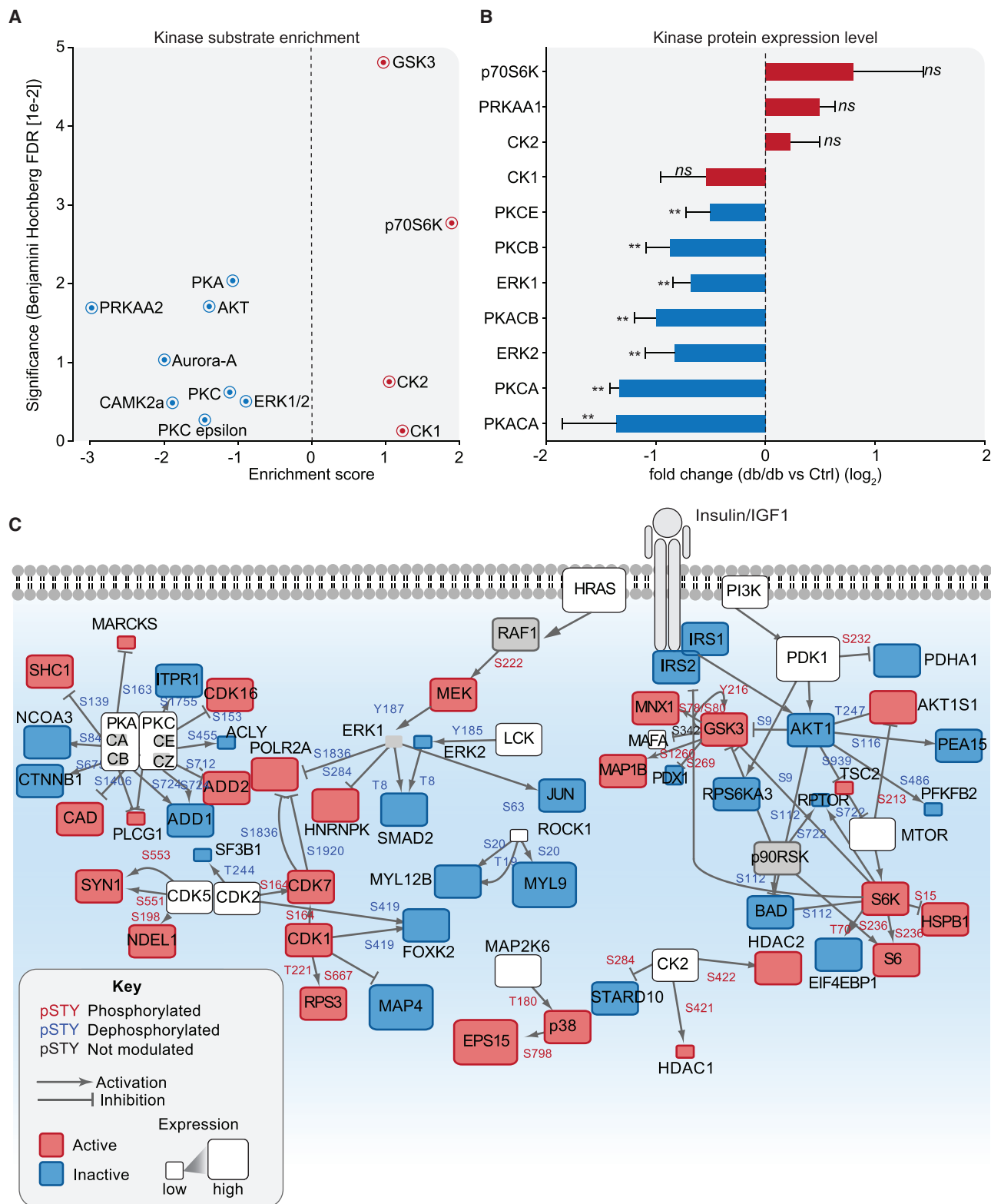
Figure 2. Key Signaling Pathways Are Modulated in db/db Islets

(A) Kinase substrate motifs significantly overrepresented in significantly modulated phosphosites in db/db islets (Benjamini-Hochberg FDR < 0.05).

(B) Log2 fold change of the expression levels of the indicated kinases in db/db islets with respect to control islets.

We next compared our dataset to previous proteomic studies of proteome remodeling in pancreatic islets of murine and rat T2D models. In insulin-resistant MKR mice, only 159 regulated proteins had been reported (Lu et al., 2008); however, 45% of them were also regulated in our much deeper dataset (Figure S4A). Likewise, in a study of ob/ob and high-fat-diet mice (El Ouaamari et al., 2015), 198 of the 272 significantly regulated proteins were likewise found in our set. In addition to the highly significant overlap in protein identifications, quantitative correlation with our study was also relatively high (Pearson's correlations 0.7 to 0.83) (Figures S4B and S5A–S5D). In contrast, the 2,372 regulated proteins in non-obese GK rats (Hou et al., 2017) were less well correlated, although they still significantly overlapped with our data (35%; p < 0.05). We attribute this to the fact that the previous models all involve obesity and insulin resistance, whereas beta cell failure is apparently quite different in the GK model. Interestingly, a large fraction of the 107 genes significantly modulated in islets derived from all four different T2D models were involved in the ER stress response (FDR < 0.05; Figures S4C and S5E). Glucolipotoxicity triggers the accumulation of misfolded proteins that are removed from the ER and subjected to ER-associated degradation (ERAD). Misfolded proteins are translocated to the cytosol, ubiquitylated, and degraded in the proteasome (Karunakaran et al., 2012). Thus, these unbiased proteomic screens suggest that the upregulation of different components of the ubiquitin/proteasome system is a major common adaptation mechanism of type 2 diabetic islets to glucolipotoxicity caused by the accumulation of misfolded proteins.

GWASs have identified several DNA loci associated with T2D (Scott et al., 2017); however, whether and how these genetic variants lead to changes in gene expression and are functionally connected to T2D generally remains unclear. We observed a significant overlap between genes carrying SNPs in T2D patients and db/db modulated proteins: more than 60% of the GWAS genes quantified at the protein level by our screen were significantly modulated (Figure S4D). This suggests that protein levels might in some cases be linked to DNA variants of the respective gene products by affecting gene expression, protein stability, or degradation. This connection also implies that some of the proteins differentially expressed in the islets of this mouse model of T2D may also be affected in islets of T2D patients. Additionally, we compared our proteomic dataset to a recently published transcriptome study in which the gene expression profile of islets isolated from db/+ and db/db 12-week-old mice was reported (Neelankal John et al., 2018). In addition to a great overlap of identification (62%), the Pearson's correlation coefficient between the transcriptome and our proteome data was 0.6, which is at the upper end of proteome and transcriptome comparisons in general (Figure S6A). To broaden our analysis, we characterized which biological processes were most altered in db/db islets, and at which of three molecular levels (transcriptome, proteome, or phosphoproteome). While pathways involved in cell cycle and

insulin secretion were downregulated at both transcriptome and proteome levels in T2D islets, metabolic pathways, including oxidative phosphorylation (OxPhos), respiratory chain, and mitochondria, were all significantly downregulated at the proteome and phosphoproteome levels (Figure S6B).

Drastic Remodeling of the Proteome and Phosphoproteome in db/db Islets

Around 35% of the proteome was modulated in db/db islets at an FDR <0.07 (Figures S7A and S8A; Table S1) and more than 25% of phosphopeptides on over 40% of phosphoproteins (Figures S7B, S8B, and S8C; Table S2). Interestingly, the levels of 72% of these phosphopeptides are increased in db/db with respect to control islets. We interpret this observation to reflect a more active global signaling due to the high nutrition state.

Combined analysis of the phosphoproteome and proteome data showed that phosphorylation sites were evenly detected, irrespective of protein abundance, and that for 82% of the quantified phosphorylation sites, the corresponding protein was also quantified (Figures S3C–S3E and S8D). When normalizing for the protein levels, more than 60% of sites were still significantly regulated, while the regulation of the remaining proteins was due to a combination of changing phosphorylation and protein levels. In 65% of those cases, phosphorylation and protein levels both increased (46%) or decreased (18%) (Figure S8E). Together, our data reveal that a full third of the measured proteome and a quarter of the phosphoproteome are changed in our diabetes model. This result also highlights the need for joint analysis of protein and phosphorylation changes for a complete view of the molecular changes underlying pancreatic islet dysfunction.

We next asked which biological processes were most altered in db/db islets and at which molecular level. For the proteome, a strong downregulation of proteins involved in insulin secretion (at least 2-fold and up to 100-fold) correlated with an impairment of mitochondrial metabolic processes, such as TCA cycle and OxPhos, and with an increased lipid metabolism (Figures S7C and S8F). Downregulation of annotated insulin secretion proteins was also associated with increased ER and oxidative stress. Interestingly, db/db islets showed a positive enrichment of proteins involved in cell-cell adhesion and cell migration. At the signaling level, the mTOR pathway and autophagy, a downstream process, were positively enriched in db/db islets (Figure S8F). These changes occurred only at the phosphoproteome level and will be discussed in more detail below.

Key Signaling Pathways Are Remodeled in Diabetic Islets

To investigate the mechanisms responsible for the phosphoproteome level changes, we extracted the kinase substrate motifs (Keshava Prasad et al., 2009) significantly changed in db/db islets (Figure 2A) (Fisher's exact test, FDR < 0.05; STAR Methods). Consistent with high nutrient-induced mTOR hyperactivation,

---

(C) The phosphoproteome and proteome changes observed in db/db islets were mapped onto a literature-curated signaling network. Node size is proportional to the protein expression change in db/db islets. Blue and red nodes are inactivated or activated in db/db islets, respectively. Phosphorylation and de-phosphorylation reactions on specific residues are represented as edges between nodes. Phosphosites are colored according to their phosphorylation state in db/db islets, as indicated in the legend.

the substrate motif of p70S6K (itself a direct target of mTORC1) was enriched, while the AMPK motif was downregulated. Other key kinase motifs, such as those of ERK1/2 and AKT, were also downregulated. Additionally, the substrate motifs of key kinases previously implicated in the regulation of insulin secretion, including PKA, PKC, and CaMK (Sacco et al., 2016a; Shibasaki et al., 2007), were downregulated, further explaining the inability of diabetic beta cells to properly secrete insulin after glucose stimulation. Enrichment or depletion of a specific substrate motif may be the consequence of the modulation of kinase activity or protein concentration and the proteome levels can help to unravel this question. We observed all of the catalytic subunits of PKA and PKC to be consistently downregulated in db/db islets, as well as the MAPKs ERK1 and ERK2 (Figure 2B).

As our data clearly indicate that key kinases are modulated in db/db islets, we next wanted to understand how signaling pathways are globally rewired in conditions of beta cell failure. We previously developed an approach that integrates large-scale quantitative phosphoproteomic and proteomic data with a literature-derived, proteome-wide signaling network (Sacco et al., 2016b). Exploration of the activation/inactivation pattern in the resulting graph confirmed and extended our previous observations, highlighting that all PKA and PKC substrates in our dataset were significantly dephosphorylated in the db/db islets, and that the expression levels of the PKA and PKC catalytic subunits were also decreased (Figure 2C). Several G protein-coupled receptors, including Gpr119, Glp1, and Gpr40, have attracted considerable interest as T2D drug targets, due to their potential positive effects on insulin secretion via indirect activation of PKA and PKC (Bailey et al., 2016). Our data indicate that PKA and PKC are downregulated, strongly suggesting that drug efficacy considerations should take the results of proteomics measurements into account.

Interestingly, we found that phosphorylation of the activating residue Thr8 of the SMAD2 transcription factor, which leads to its inactivation (Funaba et al., 2002), was significantly decreased. Consistently, Smad2βKO (knockout) mice have striking islet hyperplasia together with defective glucose-responsive insulin secretion (Nomura et al., 2014).

The high-nutrient-induced mTOR hyperactivation that we observed in diabetic islets leads to inhibition of AKT through the well-characterized p70S6K-IRS1/2 negative feedback loop (Hsu et al., 2011). Decreased AKT activity in turn decreases phosphorylation of its direct substrate, the inhibitory Ser9 of GSK3beta, which we indeed observed in our dataset. Likewise, phosphorylation of the activating Tyr216 of GSK3beta was significantly increased, further confirming increased GSK3beta activity in db/db islets. Ser269 of the key beta cell-specific transcription factor PDX1 is a direct substrate of GSK3beta and HIPK2, and phosphorylation of this residue causes its proteasomal degradation (Humphrey et al., 2010; An et al., 2010). While the phosphorylation of the Ser269 of PDX1 was increased (Figure S9A) and the protein level of PDX1 impaired in db/db islets (Figure S9C), the mRNA level of PDX1 was not affected (Figure S9B). Our joined literature and proteomic network suggest a signaling axis starting from mTOR hyperactivation, GSK3beta activation (HIPK2 was not modulated in db/db islets), and PDX1 degradation, whose functional role in diabetic islets we investigate below.

PDX1 Suppression Downregulates GLUT2 and Inhibits Beta Cell Glycolysis in db/db Islets

Given our finding that GSK3beta is hyperactivated in diabetic islets, leading to PDX1 degradation and the established importance of PDX1 in beta cell physiology, we asked whether the expression of downstream targets of PDX1 were also impaired in beta cells. Such targets include well-characterized beta cell markers, such as the glycolytic enzyme glucokinase, the insulin genes, the major murine islet glucose transporter GLUT2, and the transcription factors NKX6.1 and HNF4A (Gao et al., 2014). Remarkably, all of these PDX1 targets were significantly downregulated in db/db islets (except for HNF4A, which we did not identify), with GLUT2 protein levels drastically decreasing by 64-fold in db/db islets compared to control islets (Figure 3A). We hypothesized that the strong reduction of GLUT2 with respect to the other beta cell markers may indicate a different, specific regulatory mechanism, but also explored the possibility that the cellularity of diabetic islets may be affected: for instance, a decreased beta cell population with the concomitant increase of other islet cell types such as alpha cells. A comprehensive analysis of the literature allowed us to monitor the changes in the expression level of 13 canonical and 70 newly identified potential markers of alpha, beta, delta, and PP cells in our diabetic islets. With the exception of the PDX1-controlled genes and GLP1R, the remaining beta cell markers were not decreased in diabetic islets (Figure S10). Additionally, we did not observe any significant modulation of alpha, delta, epsilon, and PP cell markers (Figure S10), indicating that the balance between islet cell populations is not affected in diabetic islets. Together these observations show that beta cells are not modulated in their abundance, and that the observed changes are due to a drastically remodeled proteome.

In diabetic islets, we observed a drastic reduction of GLUT2, which is the only glucose transporter detected in normal pancreatic islets and therefore has a crucial role in the insulin secretion pathway. In the absence of GLUT2, there is no compensatory expression of either GLUT1 and GLUT3 in islets (Guillam et al., 2000), and accordingly, our in-depth proteomic analysis detected neither GLUT1 nor GLUT3. Decreased expression of GLUT2 strongly impairs glucose's ability to affect insulin biosynthesis and secretion, and this correlates with a strong impairment of whole-body glucose utilization (Guillam et al., 2000). Consistently, our combined proteomic and literature mining approach revealed that in db/db islets most of the key enzymes involved in glycolysis and the TCA cycle were significantly downregulated, globally impairing glucose metabolism (Figure 3B). In particular, we observed that the expression levels of almost all the subunits of the respiratory enzymes were also significantly decreased—by 2-fold on average. The decreased glycolytic metabolism should lead to a lower [ATP]/[ADP] concentration ratio, which should negatively affect downstream components of the insulin secretion machinery. Indeed, the proteomics data indicated a significant downregulation of many proteins involved in insulin granules exocytosis (Figure 3B; Table S1). Thus, our data provide a molecular explanation for the insulin secretion failure observed in islets from 10- to 13-week-old db/db mice (Do et al., 2014; Guan et al., 2016; Kim et al., 2015; Kondo et al., 2012). The lower [ATP]/[ADP] concentration ratio in db/db islets should promote AMPK activation, which is likely to
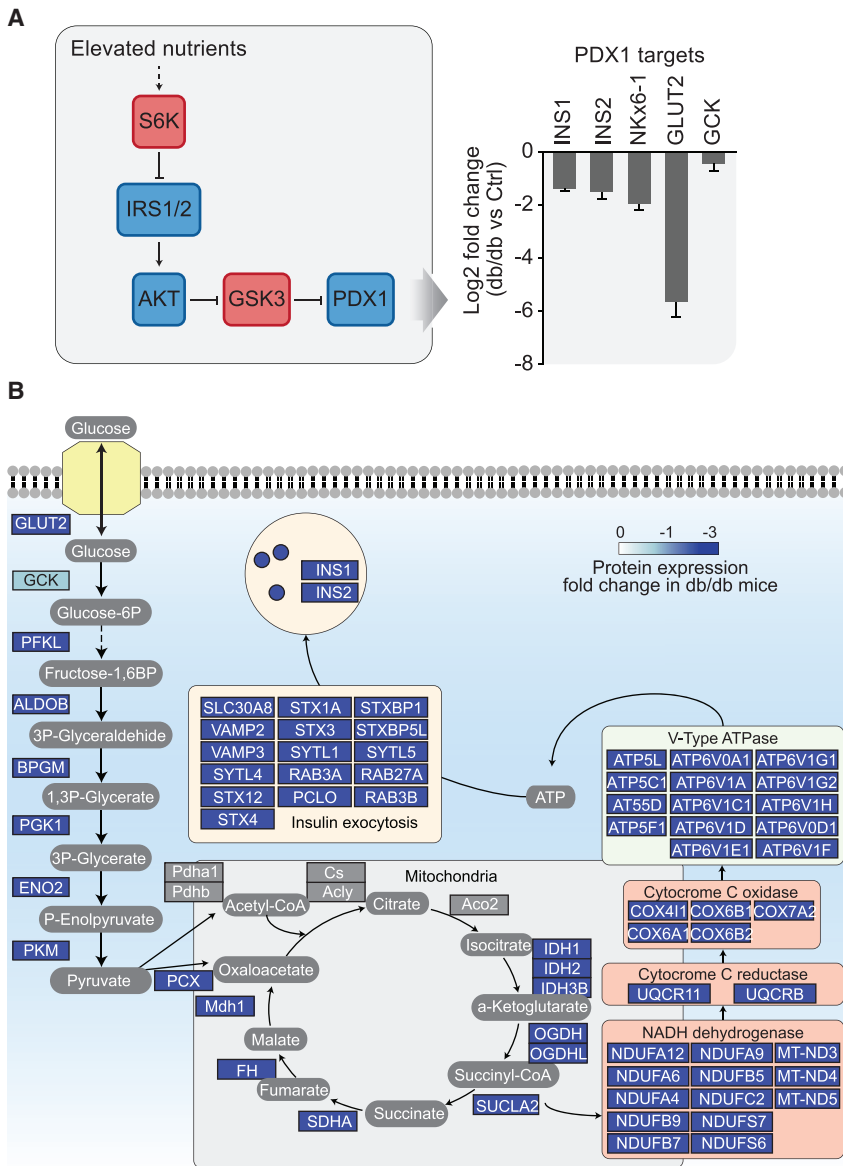
consequent degradation of PDX1 transcription factor and its targets.

We chronically treated human islets from three different donors (Figure 4A) as well as INS1e rat beta cells with high glucose and applied our MS-based proteomic and phosphoproteomic workflows to study global changes (Figure S10A). This enabled the reproducible quantification of around 7,000 proteins and 19,000 phosphosites and their response to chronically elevated glucose levels (Figures 4A, S11A, S11E, and S11F; Tables S3 and S4). To investigate and interpret the activation status of the PI3K-AKT-GSK3 and other key signaling pathways, we again integrated our datasets with the literature-derived signaling network. This revealed that chronic hyperglycemia leads to GSK3 hyperactivation in both human islets and rat beta cells (Figures 4B and S11B). We also observed the subsequent phosphorylation increase of the GSK3 target, Ser268 PDX1, causing its degradation, as evidenced by its decreased protein levels (Figure 4B). These observations were further confirmed in INS1e cells chronically treated with high glucose (Figure S11B). The expression levels of the identified PDX1 targets, including GLUT2 and INS, were decreased, as they had been in db/db islets (Figures 4C and S11C). Likewise, PDX1 suppression was again correlated with suppression of proteins involved in glucose metabolism, TCA cycle, OxPhos, and insulin secretion (Figure S11D).

Next, we wished to verify a key functional role of GSK3 in the regulation of PDX1 stability and therefore its transcriptional target GLUT2. First, we activated GSK3-treated human islets by inhibiting PI3K, either alone or in the presence of the proteasome inhibitor MG132. Indeed, GSK3 activation was sufficient to cause PDX1 degradation and GLUT2 suppression (Figures S12A–S12C, S13A, and S13B). Importantly, GSK3 activation also impaired glucose-stimulated insulin secretion (Figure S13A). These effects were completely abrogated by co-treatment with the proteasome inhibitor. We next asked whether the pharmacological inhibition of GSK3 could rescue key diabetic features of obese mice. Remarkably, treatment with LY2090314, a specific, well-characterized GSK3 inhibitor currently in clinical trials for

be inhibited (Figure 2A). This observation suggests that other potential mTOR-dependent mechanisms are responsible for AMPK inhibition in db/db islets.

Glucotoxicity Triggers the GSK3-Dependent Downregulation of PDX1

During T2D, different factors synergistically contribute to beta cell loss and dysfunction. Chronic or recurrent exposure of the beta cell leads to elevated levels of glucose and lipids (glucolipotoxicity) or to proinflammatory cytokines that interfere with beta cell function, contributing to their destruction (Prentki and Nolan, 2006). GSK3beta regulates glucose homeostasis (Humphrey et al., 2010) and our data implicate its hyperactivation in PDX1 suppression, which in turn leads to an impairment of insulin secretion machinery in db/db islets. Therefore, we next investigated whether glucotoxicity in isolation triggers GSK3beta activation in the beta cell leading to
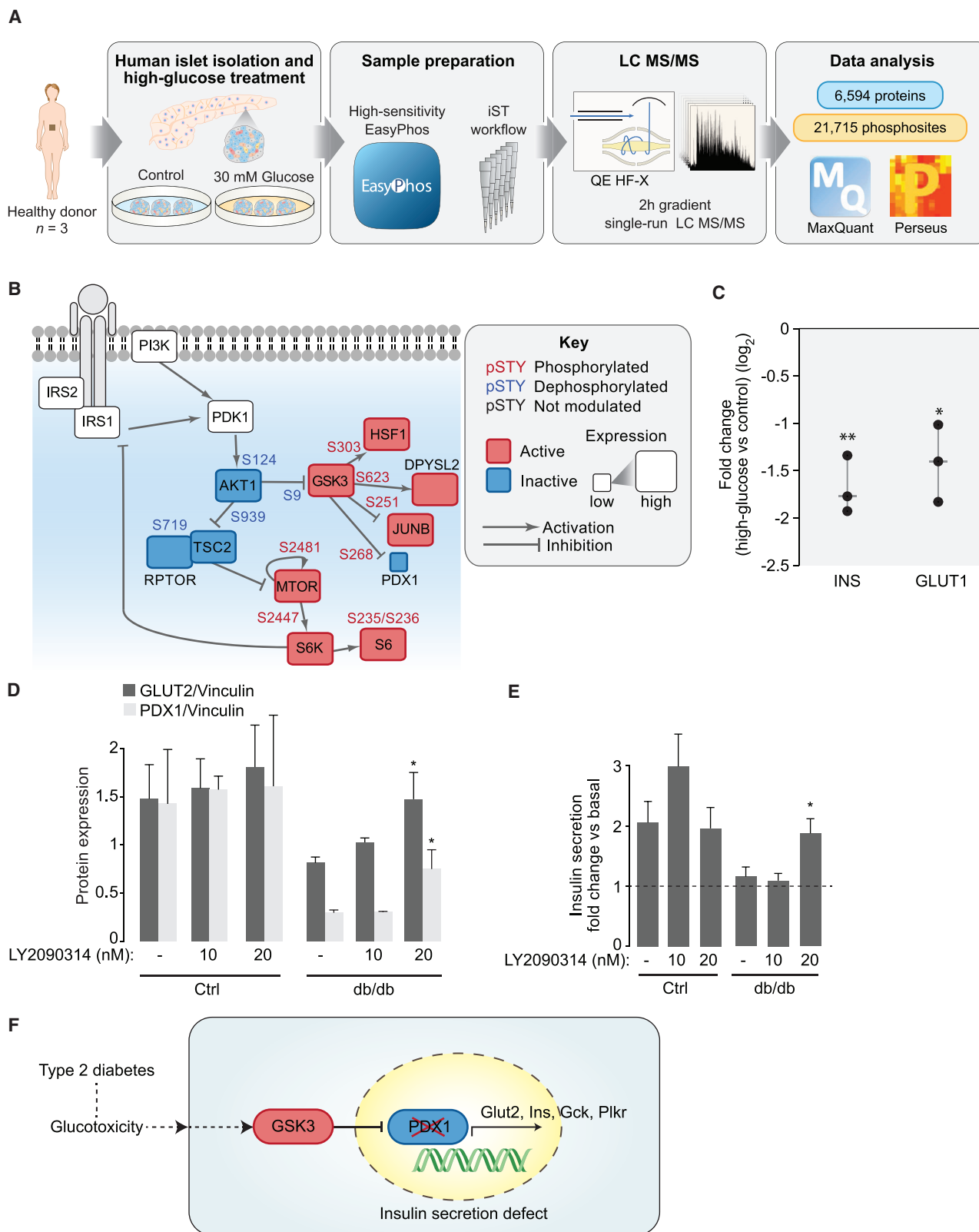
Figure 4. Glucotoxicity Triggers GSK3-Dependent PDX1 Degradation

(A) Schematic representation of the experimental workflow applied to analyze the proteome and phosphoproteome of human islets after chronic high-glucose stimulation.

(legend continued on next page)

the treatment of melanoma, not only restored the expression level of GLUT2 and PDX1, but also almost completely rescued the ability of diabetic islets to properly respond to glucose stimulation by secreting insulin (Figure 4D). LY2090314 treatment did not affect PDX1 mRNA level (Figure S14), excluding an indirect mechanism through gene expression regulation.

Conclusion

Complex diseases are rarely caused by an abnormality in a single gene, but rather by perturbations of global cellular networks. Investigating the rewiring of signaling networks in diabetic islets has been a major goal in diabetes research; however, this has so far been prevented by the extremely limited amount of material that can be extracted from these structures that are composed of just a few thousand cells. Applying a newly developed, highly sensitive phosphoproteomic workflow, we here obtained a very detailed portrait of the dynamic changes in protein expression and phosphorylation in obese diabetic mice. Integrating of this large-scale dataset with literature-derived signaling pathways revealed how misregulated proteins and signaling events contribute to islet dysfunction. Chief among these was the hyperactivation of the kinase GSK3 in db/db islets, and we discovered that its functional role in the regulation of insulin secretion involves a PDX1-dependent mechanism. Together, our global proteomics and phosphoproteomic data, combined with functional data, support a model whereby a diabetic environment, including chronic hyperglycemia and associated glucotoxicity, leads to beta cell failure at least in part through a GSK3-PDX1-dependent axis (Figure 4F). This mechanism also provides a molecular explanation for the already discovered beneficial effects of GSK3 inhibitors in T2D treatment (MacAulay and Woodgett, 2008; Stein et al., 2011). Further in-depth exploration of the resource provided here may aid in the discovery of other potential islet-related diagnostic and therapeutic targets for human T2D.

Limitations of Study

A number of important additional challenges remain to apply our findings in the field of T2D research. First, our study employed T2D murine islets and human islets from three different islet donors. This observation reflects the difficulty of accessing human diabetic and healthy islets. Additionally, existing models of cell lines of healthy and diabetic conditions are not perfect, limiting the possibility to perform high-throughput drug screening.

Our study identifies GSK3 inhibitors as promising therapeutic agents to restore the ability of beta cells to secrete insulin in T2D. However, specifically targeting inhibition to beta cells would likely be beneficial but poses a major challenge. As GSK3 is ubiquitously expressed, GSK3 inhibition could potentially have off-targets effects in other tissues. Although GSK3 inhibitors are currently tested in melanoma patients where no major off-target effects have been observed, this issue needs to be further explored in T2D patients. It will be interesting to identify beta cell-

specific proteins that are involved in the modulation of GSK3 activity. Targeting these would be an elegant way to develop beta cell-specific drugs that restore beta cell functionality in T2D.

STAR★METHODS

Detailed methods are provided in the online version of this paper and include the following:

- KEY RESOURCES TABLE
- CONTACT FOR REAGENT AND RESOURCE SHARING
- EXPERIMENTAL MODEL AND SUBJECT DETAILS
  - Ethics Statement
  - Human Islet Isolation and Culture
  - Animals and Islet Isolation
- METHOD DETAILS
  - Insulin Assay
  - Proteome and Phosphoproteome Sample Preparation
  - Mass Spectrometric Analyses
  - Cell Culture
  - RNA Extraction, Retro-transcription, Real Time PCR and Analysis
  - Immunofluorescence Microscopy
- QUANTIFICATION AND STATISTICAL ANALYSIS
  - Proteome and Phosphoproteome Data processing
  - Proteome and Phosphoproteome Bioinformatics Data Analysis
  - GWAS Data Comparison with Our Proteomic Data
  - Combining Proteome and Phosphoproteome Data with a Prior Knowledge Signaling Network
- DATA AND SOFTWARE AVAILABILITY

AUTHOR CONTRIBUTIONS

F.S. conceived and M.M. supervised the project. F.S. performed the proteome, phosphoproteome, immunofluorescence, and insulin secretion analyses. A.S. and F.V. dissected mice, isolated islets, and performed the insulin secretion assay. P.M. provided human islets and revised the manuscript. N.K. measured the last batch of proteome samples and the human islet proteome and phosphoproteome. S.J.H. optimized the workflow for phosphoproteome islet analysis. A.R. helped in the GSK3 inhibition experiments. F.S. analyzed the data. F.S., N.K., S.J.H., J.G., and M.M. wrote the manuscript.

DECLARATION OF INTERESTS

The authors declare no competing interests.

(B) Proteome and phosphoproteome datasets were overlaid onto a literature-derived signaling network.
(C) Log2 protein expression fold change of PDX1 and its transcriptional targets.
(D) Bar graph of GLUT2 and PDX1 protein levels normalized on the loading control in db/db and control islets in the indicated experimental conditions.
(E) Amount of secreted insulin reported as fold change on basal condition in db/db and control islets in the indicated experimental conditions.
(F) A proposed model contributing to glucotoxicity-dependent beta cell failure.

REFERENCES

Ahlqvist, E., Storm, P., Käräjämäki, A., Martinell, M., Dorkhan, M., Carlsson, A., Vikman, P., Prasad, R.B., Aly, D.M., Almgren, P., et al. (2018). Novel subgroups of adult-onset diabetes and their association with outcomes: a data-driven cluster analysis of six variables. Lancet Diabetes Endocrinol. *6*, 361–369.

An, R., da Silva Xavier, G., Semplici, F., Vakhshouri, S., Hao, H.-X.X., Rutter, J., Pagano, M.A., Meggio, F., Pinna, L.A., and Rutter, G.A. (2010). Pancreatic and duodenal homeobox 1 (PDX1) phosphorylation at serine-269 is HIPK2-dependent and affects PDX1 subnuclear localization. Biochem. Biophys. Res. Commun. *399*, 155–161.

Bailey, C.J., Tahrani, A.A., and Barnett, A.H. (2016). Future glucose-lowering drugs for type 2 diabetes. Lancet Diabetes Endocrinol. *4*, 350–359.

Blandino-Rosano, M., Chen, A.Y., Scheys, J.O., Alejandro, E.U., Gould, A.P., Taranukha, T., Elghazi, L., Cras-Méneur, C., and Bernal-Mizrachi, E. (2012). mTORC1 signaling and regulation of pancreatic β-cell mass. Cell Cycle *11*, 1892–1902.

Chen, H., Charlat, O., Tartaglia, L.A., Woolf, E.A., Weng, X., Ellis, S.J., Lakey, N.D., Culpepper, J., Moore, K.J., Breitbart, R.E., et al. (1996). Evidence that the diabetes gene encodes the leptin receptor: identification of a mutation in the leptin receptor gene in db/db mice. Cell *84*, 491–495.

Cox, J., and Mann, M. (2008). MaxQuant enables high peptide identification rates, individualized p.p.b.-range mass accuracies and proteome-wide protein quantification. Nat. Biotechnol. *26*, 1367–1372.

Cox, J., and Mann, M. (2012). 1D and 2D annotation enrichment: a statistical method integrating quantitative proteomics with complementary high-throughput data. BMC Bioinformatics *13* (Suppl 16), S12.

DeFronzo, R.A., Ferrannini, E., Groop, L., Henry, R.R., Herman, W.H., Holst, J.J., Hu, F.B., Kahn, C.R., Raz, I., Shulman, G.I., et al. (2015). Type 2 diabetes mellitus. Nat. Rev. Dis. Primers *1*, 15019.

Do, O.H., Low, J.T., Gaisano, H.Y., and Thorn, P. (2014). The secretory deficit in islets from db/db mice is mainly due to a loss of responding beta cells. Diabetologia *57*, 1400–1409.

Donath, M.Y., Dalmas, É., Sauter, N.S., and Böni-Schnetzler, M. (2013). Inflammation in obesity and diabetes: islet dysfunction and therapeutic opportunity. Cell Metab. *17*, 860–872.

El Ouaamari, A., Zhou, J.Y., Liew, C.W., Shirakawa, J., Dirice, E., Gedeon, N., Kahraman, S., De Jesus, D.F., Bhatt, S., Kim, J.S., et al. (2015). Compensatory islet response to insulin resistance revealed by quantitative proteomics. J. Proteome Res. *14*, 3111–3122.

Funaba, M., Zimmerman, C.M., and Mathews, L.S. (2002). Modulation of Smad2-mediated signaling by extracellular signal-regulated kinase. J. Biol. Chem. *277*, 41361–41368.

Gao, T., McKenna, B., Li, C., Reichert, M., Nguyen, J., Singh, T., Yang, C., Pannikar, A., Doliba, N., Zhang, T., et al. (2014). Pdx1 maintains β cell identity and function by repressing an α cell program. Cell Metab. *19*, 259–271.

Guan, S.S., Sheu, M.L., Yang, R.S., Chan, D.C., Wu, C.T., Yang, T.H., Chiang, C.K., and Liu, S.H. (2016). The pathological role of advanced glycation end products-downregulated heat shock protein 60 in islet β-cell hypertrophy and dysfunction. Oncotarget *7*, 23072–23087.

Guillam, M.T., Dupraz, P., and Thorens, B. (2000). Glucose uptake, utilization, and signaling in GLUT2-null islets. Diabetes *49*, 1485–1491.

Hornbeck, P.V., Zhang, B., Murray, B., Kornhauser, J.M., Latham, V., and Skrzypek, E. (2015). PhosphoSitePlus, 2014: mutations, PTMs and recalibrations. Nucleic Acids Res. *43*, D512–D520.

Hou, J., Li, Z., Zhong, W., Hao, Q., Lei, L., Wang, L., Zhao, D., Xu, P., Zhou, Y., Wang, Y., and Xu, T. (2017). Temporal transcriptomic and proteomic landscapes of deteriorating pancreatic islets in type 2 diabetic rats. Diabetes *66*, 2188–2200.

Hsu, P.P., Kang, S.A., Rameseder, J., Zhang, Y., Ottina, K.A., Lim, D., Peterson, T.R., Choi, Y., Gray, N.S., Yaffe, M.B., et al. (2011). The mTOR-regulated phosphoproteome reveals a mechanism of mTORC1-mediated inhibition of growth factor signaling. Science *332*, 1317–1322.

Humphrey, R.K., Yu, S.M., Flores, L.E., and Jhala, U.S. (2010). Glucose regulates steady-state levels of PDX1 via the reciprocal actions of GSK3 and AKT kinases. J. Biol. Chem. *285*, 3406–3416.

Humphrey, S.J., Azimifar, S.B., and Mann, M. (2015). High-throughput phosphoproteomics reveals in vivo insulin signaling dynamics. Nat. Biotechnol. *33*, 990–995.

Humphrey, S.J., Karayel, O., James, D.E., and Mann, M. (2018). High-throughput and high-sensitivity phosphoproteomics with the EasyPhos platform. Nat. Protoc. *13*, 1897–1916.

Kahn, S.E., Hull, R.L., and Utzschneider, K.M. (2006). Mechanisms linking obesity to insulin resistance and type 2 diabetes. Nature *444*, 840–846.

Karunakaran, U., Kim, H.J., Kim, J.Y., and Lee, I.K. (2012). Guards and culprits in the endoplasmic reticulum: glucolipotoxicity and β-cell failure in type II diabetes. Exp. Diabetes Res. *2012*, 639762.

Kelstrup, C.D., Bekker-Jensen, D.B., Arrey, T.N., Hogrebe, A., Harder, A., and Olsen, J.V. (2018). Performance evaluation of the Q Exactive HF-X for shotgun proteomics. J. Proteome Res. *17*, 727–738.

Keshava Prasad, T.S., Goel, R., Kandasamy, K., Keerthikumar, S., Kumar, S., Mathivanan, S., Telikicherla, D., Raju, R., Shafreen, B., Venugopal, A., et al. (2009). Human Protein Reference Database–2009 update. Nucleic Acids Res. *37*, D767–D772.

Kim, K.S., Jung Yang, H., Lee, I.S., Kim, K.H., Park, J., Jeong, H.S., Kim, Y., Ahn, K.S., Na, Y.C., and Jang, H.J. (2015). The aglycone of ginsenoside Rg3 enables glucagon-like peptide-1 secretion in enteroendocrine cells and alleviates hyperglycemia in type 2 diabetic mice. Sci. Rep. *5*, 18325.

Kondo, T., Sasaki, K., Matsuyama, R., Morino-Koga, S., Adachi, H., Suico, M.A., Kawashima, J., Motoshima, H., Furukawa, N., Kai, H., and Araki, E. (2012). Hyperthermia with mild electrical stimulation protects pancreatic β-cells from cell stresses and apoptosis. Diabetes *61*, 838–847.

Kulak, N.A., Pichler, G., Paron, I., Nagaraj, N., and Mann, M. (2014). Minimal, encapsulated proteomic-sample processing applied to copy-number estimation in eukaryotic cells. Nat. Methods *11*, 319–324.

Lu, H., Yang, Y., Allister, E.M., Wijesekara, N., and Wheeler, M.B. (2008). The identification of potential factors associated with the development of type 2 diabetes: a quantitative proteomics approach. Mol. Cell. Proteomics *7*, 1434–1451.

MacAulay, K., and Woodgett, J.R. (2008). Targeting glycogen synthase kinase-3 (GSK-3) in the treatment of type 2 diabetes. Expert Opin. Ther. Targets *12*, 1265–1274.

Marchetti, P., Suleiman, M., and Marselli, L. (2018). Organ donor pancreases for the study of human islet cell histology and pathophysiology: a precious and valuable resource. Diabetologia *61*, 770–774.

McCarthy, M.I., and Hattersley, A.T. (2008). Learning from molecular genetics: novel insights arising from the definition of genes for monogenic and type 2 diabetes. Diabetes *57*, 2889–2898.

Neelankal John, A., Ram, R., and Jiang, F.X. (2018). RNA-seq analysis of islets to characterise the dedifferentiation in type 2 diabetes model mice db/db. Endocr. Pathol. *29*, 207–221.

Nomura, M., Zhu, H.L., Wang, L., Morinaga, H., Takayanagi, R., and Teramoto, N. (2014). SMAD2 disruption in mouse pancreatic beta cells leads to islet hyperplasia and impaired insulin secretion due to the attenuation of ATP-sensitive K+ channel activity. Diabetologia *57*, 157–166.

Perfetto, L., Briganti, L., Calderone, A., Cerquone Perpetuini, A., Iannuccelli, M., Langone, F., Licata, L., Marinkovic, M., Mattioni, A., Pavlidou, T., et al. (2016). SIGNOR: a database of causal relationships between biological entities. Nucleic Acids Res. *44* (D1), D548–D554.

Prasad, R.B., and Groop, L. (2015). Genetics of type 2 diabetes-pitfalls and possibilities. Genes (Basel) *6*, 87–123.

Prentki, M., and Nolan, C.J. (2006). Islet beta cell failure in type 2 diabetes. J. Clin. Invest. *116*, 1802–1812.

Sacco, F., Gherardini, P.F., Paoluzi, S., Saez-Rodriguez, J., Helmer-Citterich, M., Ragnini-Wilson, A., Castagnoli, L., and Cesareni, G. (2012). Mapping the human phosphatome on growth pathways. Mol. Syst. Biol. *8*, 603.

Sacco, F., Humphrey, S.J., Cox, J., Mischnik, M., Schulte, A., Klabunde, T., Schäfer, M., and Mann, M. (2016a). Glucose-regulated and drug-perturbed phosphoproteome reveals molecular mechanisms controlling insulin secretion. Nat. Commun. *7*, 13250.

Sacco, F., Silvestri, A., Posca, D., Pirrò, S., Gherardini, P.F., Castagnoli, L., Mann, M., and Cesareni, G. (2016b). Deep proteomics of breast cancer cells reveals that metformin rewires signaling networks away from a pro-growth state. Cell Syst. *2*, 159–171.

Saisho, Y. (2015). β-cell dysfunction: its critical role in prevention and management of type 2 diabetes. World J. Diabetes *6*, 109–124.

Scott, R.A., Scott, L.J., Mägi, R., Marullo, L., Gaulton, K.J., Kaakinen, M., Pervjakova, N., Pers, T.H., Johnson, A.D., Eicher, J.D., et al.; DIAbetes Genetics Replication And Meta-analysis (DIAGRAM) Consortium (2017). An expanded genome-wide association study of type 2 diabetes in Europeans. Diabetes *66*, 2888–2902.

Segerstolpe, Å., Palasantza, A., Eliasson, P., Andersson, E.M., Andréasson, A.C., Sun, X., Picelli, S., Sabirsh, A., Clausen, M., Bjursell, M.K., et al. (2016). Single-cell transcriptome profiling of human pancreatic islets in health and type 2 diabetes. Cell Metab. *24*, 593–607.

Sharma, K., D'Souza, R.C., Tyanova, S., Schaab, C., Wiśniewski, J.R., Cox, J., and Mann, M. (2014). Ultradeep human phosphoproteome reveals a distinct regulatory nature of Tyr and Ser/Thr-based signaling. Cell Rep. *8*, 1583–1594.

Shibasaki, T., Takahashi, H., Miki, T., Sunaga, Y., Matsumura, K., Yamanaka, M., Zhang, C., Tamamoto, A., Satoh, T., Miyazaki, J., and Seino, S. (2007). Essential role of Epac2/Rap1 signaling in regulation of insulin granule dynamics by cAMP. Proc. Natl. Acad. Sci. USA *104*, 19333–19338.

Stein, J., Milewski, W.M., Hara, M., Steiner, D.F., and Dey, A. (2011). GSK-3 inactivation or depletion promotes β-cell replication via down regulation of the CDK inhibitor, p27 (Kip1). Islets *3*, 21–34.

Tyanova, S., Temu, T., Sinitcyn, P., Carlson, A., Hein, M.Y., Geiger, T., Mann, M., and Cox, J. (2016). The Perseus computational platform for comprehensive analysis of (prote)omics data. Nat. Methods *13*, 731–740.

STAR★METHODS

KEY RESOURCES TABLE

REAGENT or RESOURCE	SOURCE	IDENTIFIER
Antibodies		
PDX1 antibody	CST	RRID: AB_10706174
GLUT2 antibody	Invitrogen	RRID: AB_263321
Goat polyAb anti-Mouse IgG (H+L)-HRP	Bio-Rad	RRID: AB_11125936
Goat polyAb anti-Rabbit IgG (H+L)-HRP	Bio-Rad	RRID: AB_11125142
GSK3 (P) antibody	CST	RRID: AB_10013750
Phalloidin FITC antibody	CST	RRID: AB_2315147
Goat anti-Mouse IgG (H+L) Antibody Alexa Fluor 555	Invitrogen	RRID: AB_2535846
Goat anti-Mouse IgG (H+L) Antibody Alexa Fluor 488	Invitrogen	RRID: AB_2534069
Goat anti-Rabbit IgG (H+L) Antibody Alexa Fluor 555	SouthernBiotech	Cat# 4050-30
Goat anti-Rabbit IgG (H+L) Antibody Alexa Fluor 488	SouthernBiotech	Cat# 1012-31
Fetal Bovin Serum (FBS)	Euroclone	Cat# ECS0180L
Medium 199	GIBCO	Cat# 11150-059
Trypsin-EDTA 0.05% w/Phenol Red	Euroclone	Cat# ECM0920D
DMEM GlutaMAX	GIBCO	Cat# 61965-026
HBSS w/o Ca^{2+}, Mg^{2+}	GIBCO	Cat# 14170112
Penicillin-Streptomycin (P/S) 10000 U/mL	GIBCO	Cat# 15140122
RPMI 1640	GIBCO	Cat# 21875-091
Hoelscth 33342	Invitrogen	Cat# H3570
INS-1E cells	Dr Martin Jastroch, IDO	RRID: CVCL_0351
Human islets	CelProgen	Cat# 35002-04
Critical Commercial Assays		
Insulin assay	Cisbio Bioassays	Cat# 62INSPEC
Software and Algorithms		
GraphPad Prism	GraphPad Software	RRID: SCR_002798
Cytoscape 3.7.1	https://cytoscape.org/	RRID: SCR_003032
MaxQuant 1.5.3.6	Cox and Mann, 2008	RRID: SCR_014485
Perseus 1.6.2.3	Tyanova et al., 2016	RRID: SCR_015753

CONTACT FOR REAGENT AND RESOURCE SHARING

Requests for further information, reagents, and resources should be directed to and will be fulfilled by the Lead Contact, Matthias Mann (mmann@biochem.mpg.de).

EXPERIMENTAL MODEL AND SUBJECT DETAILS

Ethics Statement
Human islets were isolated from pancreas of nondiabetic multiorgan donors with the approval of the Ethics Committee of the University of Pisa. Human pancreas were collected from brain-dead organ donors (Marchetti et al., 2018) after informed consent was obtained in writing form from family members.

Human Islet Isolation and Culture
Human islets were isolated by enzymatic digestion and density gradient purification from pancreatic samples of multiorgan donors, as detailed elsewhere [27], [28]. Isolated islets were then cultured in M199 medium at 5.5 mmol/l glucose until experiments were performed.

Animals and Islet Isolation

13 week old C57BLKS-Leprdb homozygous and age-matched C57BLKS-Leprdb/+ heterozygous mice (Charles River Laboratories) were housed in light-tight boxes with free access to food and water and entrained to a 12 hr/12 hr light-dark. Mice were maintained in the animal facility of the Helmholtz centrum according to institutional guidelines. Mice were euthanized. The upper abdomen was incised to expose liver and intestines. The pancreas was perfused through the common bile duct with cold collagenase P (from Roche) in saline solution. The pancreas was dissected and placed into a warm collagenase saline solution for 15 min. After enzymatic digestion of the pancreatic tissue, islets were picked and left to recover at 37°C for 2 hours. For phosphoproteome preparation, islets from three different mice were pooled to obtain about 200 μg of protein lysate.

METHOD DETAILS

Insulin Assay

Islets were incubated overnight with DMEM low glucose medium, then washed with Krebs-Ringer-Buffer (NaCl 115 mM; KCl 4.7 m; KH2PO4 1.2 mM; MgSO4*7H2O 1.2 mM; NaHCO3 20 mM; HEPES 16 mM; CaCl2* 2H2O 2.56 mM; BSA 1 g/L; pH 7.4) and incubated with starvation buffer (0.5mM glucose Krebs-Ringer-Buffer) for 90 min. Islets were then incubated with high glucose medium (Krebs-Ringer-Buffer supplemented with glucose 16.7 mM). Aliquots of the supernatant were assayed for insulin content (62INSPEC, Cisbio Bioassays) according to the manufacturer's protocol. The amount of secreted insulin was calibrated against the insulin standard, according to the manufacturer's protocol and then normalized on the untreated control.

Proteome and Phosphoproteome Sample Preparation

Cells were lysed in SDC lysis buffer containing 4% (w/v) SDC, 100 mM Tris -HCl (pH 8.5). Proteome preparation was done using the in StageTip (iST) method (Kulak et al., 2014). Phosphoproteome preparation was performed as previously described (Humphrey et al., 2015, 2018). Per condition, a total of only 200 μg protein input material was lysed, alkylated and reduced in a single step. Then proteins were digested and phosphopeptides enriched with TiO_2 beads. After elution, samples were separated by HPLC in a single run (without pre-fractionations) and analyzed by mass spectrometry.

Mass Spectrometric Analyses

The peptides or phosphopeptides were desalted on StageTips and separated on a reverse phase column (50 cm, packed in-house with 1.9-μm C18- Reprosil-AQ Pur reversed-phase beads) (Dr Maisch GmbH) over 240 min or 270 min (single-run proteome and phosphoproteome analysis respectively). Eluting peptides were electrosprayed and analyzed by tandem mass spectrometry on a Q Exactive HF (Thermo Fischer Scientific) using HCD based fragmentation, which was set to alternate between a full scan followed by up to five fragmentation scans. Proteome and phosphoproteome data were processed and statistically analyzed as described in Quantification and Statistical Analysis section.

Cell Culture

INS-1E cells (RRID: CVCL_0351) were grown in a humidified atmosphere (5% CO2, 95% air at 37°C) in monolayer in modified RPMI 1,640 medium supplemented with 10% fetal calf serum, 10 mM HEPES, 100 U ml^{-1}, penicillin, 100 mg ml^{-1}, streptomycin, 1 mM sodium pyruvate, 50 mM b-mercaptoethanol (all from GIBCO) and 0.5% BSA (from Sigma). Human islets were purchased from PELO Biotech and grown according to manufacturer instructions (CelProgen cat no. 35002-04). Isolated murine islets were cultured in RPMI (21875-034, GIBCO) supplemented with 10% FBS and Penicillin/Streptomycin.

RNA Extraction, Retro-transcription, Real Time PCR and Analysis

RNA extraction was performed using the NucleoZOL reagent (Macherey-Nagel, #740404) or QIAGEN RNeasy Mini Kit (QIAGEN, #74106) according to manufacturer instructions. Retro-transcription to cDNA was performed on 1 μg of total RNA using the PrimeScript RT Reagent Kit (Perfect Real Time) (Takara, #RR037A) according to manufacturer instructions. The reaction was performed using the GeneAmp PCR System 9700 (Applied Biosystems). Real Time PCR was performed on 100 ng of cDNA using the TB Green Premix Ex Taq (Tli RNase H Plus) (Takara, #RR420A) according to manufacturer instructions. The reaction was performed using the StepOne Real-Time PCR System (Thermo Fisher Scientific) or CFX96 System (Bio-Rad).

The primers used in the work are the following:

PDX1_FWD 5′- TACAAGCTCGCTGGGATCACT −3′;
PDX1_REV 5′- GCAGTACGGGTCCTCTTGTT −3′;
Tubulin_FWD 5′- AAGCAGCAACCATGCGTGA −3′;
Tubulin_REV 5′- CCTCCCCCAATGGTCTTGTC −3′;

Relative expression was evaluated using the $2^{-\Delta\Delta Ct}$ method.

Immunofluorescence Microscopy

Human pancreatic islets from CellProgen were treated as described. Cells were fixed for 10 min in 4% paraformaldehyde (EM Sciences), washed with PBS, 0.5% Triton X-100, and permeabilized with blocking solution (0.1% Triton, 10% fetal calf serum) for 30 min. Cells were incubated, in blocking solution, with anti-GSK3 (P) (RRID: AB_10013750), anti-GLUT2, anti-PDX1 and anti FITC phalloidin (RRID: AB_2315147) for 1 h at room temperature. Cells were rinsed in PBS and incubated with secondary antibody for 30 min. Cells were stained with 4′,6-diamidino-2-phenylindole in PBS, 0.1% Triton for 5 min at room temperature. Cells were analyzed by indirect immunofluorescence microscopy.

QUANTIFICATION AND STATISTICAL ANALYSIS

Proteome and Phosphoproteome Data processing

Raw mass spectrometry data were analyzed in the MaxQuant environment (Cox and Mann, 2008), version 1.5.1.6, employing the Andromeda engine for database search. MS/MS spectra were matched against the Mus Murine UniProt FASTA database (September 2014), with an FDR of $< 1\%$ at the level of proteins, peptides and modifications. Enzyme specificity was set to trypsin, allowing for cleavage N-terminal to proline and between aspartic acid and proline. The search included cysteine carbamidomethylation as a fixed modification, and N-terminal protein acetylation, oxidation of methionine and phosphorylation of serine, threonine tyrosine residue (STY) as variable modifications. Label free proteome analysis was performed in MaxQuant. For proteome and phosphoproteome analysis, where possible, the identity of peptides present but not sequenced in a given run was obtained by transferring identifications across liquid chromatography (LC)-MS runs ('match between runs'). For phosphopeptide identification, an Andromeda minimum score and minimum delta score threshold of 40 and 17 were used, respectively. Up to three missed cleavages were allowed for protease digestion and peptides had to be fully tryptic.

Proteome and Phosphoproteome Bioinformatics Data Analysis

Bioinformatic analysis was performed in the Perseus software environment (Tyanova et al., 2016). Statistical analysis of proteome and phosphoproteome was performed on logarithmized intensities for those values that were found to be quantified in any experimental condition. Phosphoproteome intensities were normalized by subtracting the median intensity of each sample. To identify significantly modulated proteins and phosphopeptides across two different conditions, we performed a Student t-Test with a permutation-based FDR cutoff of 0.07 and S0 = 0.1. Categorical annotation was added in Perseus in the form of GO biological process (GOBP), molecular function (GOMF), and cellular component (GOCC), KEGG pathways and kinase substrate motifs (extracted from HPRD). Concerning the kinase substrate motifs, we performed a 1D annotation enrichment analyses to identify statistically significant enriched kinase-substrates motifs in db/db islets (Cox and Mann, 2012). Multiple hypothesis testing was controlled by using a Benjamini-Hochberg FDR threshold of 0.05. Then for each kinase-substrate motif the corresponding pValue and score are assigned. While a score near 1 indicates a positive enrichment, a score near -1 means a negative enrichment of the category.

GWAS Data Comparison with Our Proteomic Data

We have retrieved the list of genes with SNPs significantly (p value < 0.05) associated with type 2 diabetes by using the EBI GWAS catalog (https://www.ebi.ac.uk/gwas/search?query=Type%202%20diabetes). This provides a list of published SNP-trait associations identified by the literature and annotated by EBI curators. We have next compared this list with our proteomic data and performed the statistical analysis.

Combining Proteome and Phosphoproteome Data with a Prior Knowledge Signaling Network

This strategy has been previously developed and applied by our group (Sacco et al., 2012, 2016b). Kinase-substrate relationships were extracted by PhosphositePlus (Kinase-substrate dataset) and SIGNOR (Hornbeck et al., 2015; Perfetto et al., 2016) and were mapped onto the complete human proteome. Then the network was first filtered to maintain only relationships between proteins that were identified in our proteomic analysis of db/db islets or INS1e cells. This network was used as a scaffold to overlay the changes at the phosphoproteome level. Next the network was filtered according to the following rules: i) "leaf nodes" (connected only by one edge) whose phosphorylation was not quantified in our phospho- proteomics approach were excluded; ii) "Leaf nodes" whose phosphorylation was not modulated in db/db islets or hyperglycaemic INS1e cells were also excluded and iii) those residues (edges) whose phosphorylation status was not supported by our experimental data were eliminated. This filtering procedure yielded a much simpler network that was easier to analyze. For those proteins having multiple regulatory residues and whose phosphorylation was strongly changed in opposite direction, we considered only those sites quantified in a singly phosphorylated peptide (multiplicity = 1).

DATA AND SOFTWARE AVAILABILITY

The newly generated mass spectrometry data have been deposited in the ProteomeXchange database with the following accession number ProteomeXchange: PXD012671.